



HAL
open science

Validation of Winds Measured by MU Radar with GPS Radiosondes during the MUTSI Campaign

Hubert Luce, S. Fukao, M. Yamamoto, Claude Sidi, Francis Dalaudier

► **To cite this version:**

Hubert Luce, S. Fukao, M. Yamamoto, Claude Sidi, Francis Dalaudier. Validation of Winds Measured by MU Radar with GPS Radiosondes during the MUTSI Campaign. *Journal of Atmospheric and Oceanic Technology*, 2001, 18 (6), pp.817-829. 10.1175/1520-0426(2001)0182.0.CO;2 . hal-03124607

HAL Id: hal-03124607

<https://hal.science/hal-03124607>

Submitted on 28 Jan 2021

HAL is a multi-disciplinary open access archive for the deposit and dissemination of scientific research documents, whether they are published or not. The documents may come from teaching and research institutions in France or abroad, or from public or private research centers.

L'archive ouverte pluridisciplinaire **HAL**, est destinée au dépôt et à la diffusion de documents scientifiques de niveau recherche, publiés ou non, émanant des établissements d'enseignement et de recherche français ou étrangers, des laboratoires publics ou privés.

Validation of Winds Measured by MU Radar with GPS Radiosondes during the MUTSI Campaign

H. LUCE, S. FUKAO, AND M. YAMAMOTO

Radio Science Center for Space and Atmosphere, Kyoto University, Kyoto, Japan

C. SIDI AND F. DALAUDIER

Service d'Aéronomie du CNRS, Verrières le Buisson, France

(Manuscript received 18 August 2000, in final form 3 November 2000)

ABSTRACT

For many years, mesosphere–stratosphere–troposphere (MST) radar techniques have been used for studying the structure and dynamics of the lower and middle atmosphere. In particular, these instruments are unique tools for continuously monitoring vertical and horizontal components of the atmospheric wind at high spatial and temporal resolutions. From the very beginning, many studies have been carried out analyzing the reliability of the MST radar wind measurements and their accuracy. However, until now, very few studies have been presented confirming the high performances of the VHF Middle and upper Atmospheric (MU) radar of Japan (35°N, 136°E) for measuring the wind field. The present paper thus gives original comparisons between horizontal velocities measured by MU radar and by instrumented balloons using global positioning system (GPS) radiosondes. Twelve radiosondes were successfully used during the French–Japanese MU Radar Temperature Sheets and Interferometry (MUTSI) campaign (10–26 May 2000, Japan). They were launched about 30 km westward from the radar site, hung below capesphere-type balloons. During the campaign, two sets of radar parameters with oblique beams directed 10° and 15° off zenith at 150-m and ~2-min resolutions were used. For both configurations, a very good agreement between the two kinds of measurements was found, indicating that both wind profiles are not affected by systematic measurement biases. Moreover, the standard deviation of the differences is less than 2.6 m s⁻¹ using all radar data within a range height of 2–20 km and less than 1.5 m s⁻¹ for a radar signal-to-noise ratio larger than 0 dB in oblique directions and a horizontal radar-balloon distance smaller than 50 km. Two cases of significant differences (10–15 m s⁻¹) around the jet-stream altitude could qualitatively be explained by spatial and temporal variability of the wind field during the passage of a warm front.

1. Generalities

Originally, the stratosphere–troposphere (ST) radars were mainly dedicated to wind measurements in order to be complementary to routine meteorological rawinsondes. That is why the terminology “wind profiler” is also used, in particular for operational UHF radar network systems (e.g., Chadwick 1985). The major strength of these instruments is their capability to continuously monitor the wind speed and direction at high spatial and time resolutions. Typically, these resolutions are several hundred meters and several minutes or less, respectively. Different radar techniques have been developed for measuring the winds using either several beams (usually 3 or 5) and a single transmitting–receiving antenna array (Doppler technique) or a single vertical beam with more than 3 antenna arrays [spaced antenna (SA) techniques].

These techniques are a priori more or less influenced by aspect sensitivity at VHF (i.e., enhancement of the echo power around the zenith due to backscattering from anisotropic refractive index irregularities), gravity wave effects, and temporal and spatial intermittency of the Bragg scatterers within the radar scattering volume. The reader can refer to Hocking (1997a) for a recent review on the topic.

Large efforts have also been put forth to test the reliability and the accuracy of the different radar techniques. In the present paper, we will not dwell on this aspect for SA techniques, since the present comparisons have only been performed with radar data obtained with the Doppler technique. Tsuda et al. (1986) found that the radar oblique beams must be tilted at least 10° off zenith in order to avoid the aspect sensitivity effect with the middle and upper atmosphere (MU) radar. Indeed, an underestimate of the velocity can arise when radar beams are tilted close to the zenith because of an effective zenith angle resulting from the convolution of the antenna gain pattern and the zenith angle depen-

Corresponding author address: Dr. Hubert Luce, Radio Science Center for Space and Atmosphere, Kyoto University, Gokanoshō, Uji, Kyoto 611-0011, Japan.
E-mail: Luce@kurasc.kyoto-u.ac.jp

TABLE 1. A nonexhaustive list of previous comparisons between ST radar and rawinsonde wind measurements.

Author	Radar	Res. ^a (m)	HR ^b (km)	NC ^c
Eckund et al. (1979)	Poker Flat (49.9 MHz)	2200	6–19	2
Chang (1980)	Chatanika (1290 MHz)	750	4–14	12
Crane (1980)	(415 MHz/1320 MHz)	337/194	≈2–20	1
Fukao et al. (1980)	Arecibo (430 MHz)	600	11–28	1
Fukao et al. (1981)	Jicamarca (49.9 MHz)	2000–3000	≈20–30	4
Fukao et al. (1982)	Arecibo (430 MHz)	600	10–30	26
Larsen (1983)	Poker Flat (49.9 MHz)	Unknown	≈4–17	>60
Kato et al. (1986)	MU (46.5 MHz)	150	2–23	8
Weber and Wurtz (1990)	UHF (915 MHz)	450	≈1–9	>1000
Astin and Thomas (1992)	Aberystwyth (46.5 MHz)	600	2–16	>22
Hocking (1997b)	Clovar (40.68 MHz)	1000	2–8	29
Kishore et al. (2000)	Gadanki (53 MHz)	150	≈3.6–21	60

^a Radial resolution of the wind profiler.

^b Height range used for the comparisons.

^c Number of comparisons presented in the papers.

dence of the reflectivity (Röttger 1981). Moreover, very thin scattering layers compared to the range resolution can also produce false wind shears (e.g., Fukao et al. 1988). Because of these potential sources of errors, it is reasonable to wonder how accurate MST radars are for wind measurements.

Comparisons with in situ measurements by balloons have been carried out from the very beginning of the MST radar development. A nonexhaustive list of papers related to wind comparisons between rawinsondes and ST UHF/VHF radars is given in Table 1. The comparisons are not easy to interpret because the measurement techniques are very different. For example, the radar gives an Eulerian estimate of the wind vector integrated in volume and in time over all altitudes simultaneously and at a given location, while the balloon gives a Lagrangian value at various altitudes, at different times, and at different positions. However, the comparisons performed with routine meteorological rawinsondes as those mentioned in Table 1 are generally “fairly good” to “good,” indicating that the radar wind measurements are meaningful and can be used for meteorological applications. An interesting review of comparisons of winds measured by radar and balloons is given in Table 5 of Kishore et al. (2000). One of the most exhaustive works was presented by Weber and Würtz (1990). The authors gave statistics on data collected over many months with a 915-MHz wind profiler. After removing aberrant values produced by various interferences, they found a standard deviation of the difference between the winds measured by radar and rawinsondes of 2.5 m s⁻¹. However, these results were obtained for measurements up to ~9 km with a 450-m radar range resolution and with a radar frequency, which is not a priori concerned by aspect sensitivity. As emphasized by many authors, the largest discrepancies are often attributed to spatial and temporal inhomogeneity of the wind field. Indeed, the launching site of the balloons is sometimes very far from the radar (typically 50 km or more), and the distance of the balloon during the flight can be much

larger. Especially during disturbed meteorological conditions, such as the passage of a meteorological front or in regions with mountains, significant differences of several 10 m s⁻¹ between the two profiles can occur without any particular measurement bias in either technique. Strauch et al. (1987) and Pauley et al. (1994) studied the beam-to-beam consistency and accuracy of the wind measurements. The latter authors also compared these measurements with the results of the National Meteorological Center’s regional analysis system and found standard deviations of the difference between the wind components of 2.2 m s⁻¹ typically.

Kato et al. (1986) presented comparisons of the winds measured with the MU radar (Shigaraki, 34°51′N, 136°06′E) operating at 46.5 MHz with those measured by rawinsondes launched at meteorological stations and especially at Shionomisaki (33°30′N, 135°50′E), located at about 170 km from the radar site (see Fig. 1). The authors showed a very good agreement in wind direction. However, some noticeable differences (up to about 40 m s⁻¹) appeared in speed, with a systematic underestimate of the radar measurement when the difference occurred. In addition to the inhomogeneity of the wind field, this systematic underestimate may also be due to biases resulting from aspect sensitivity effects not reported by Tsuda et al. (1986) at 10° off zenith but argued by Astin and Thomas (1992), Hocking (1997b), Campistron et al. (1999), or Kishore et al. (2000) at smaller or larger tilt angles. The latter authors have recently performed statistics on wind velocities measured by balloons and the Indian MST radar and found a systematic underestimate of the wind measured by radar. The authors attributed this bias to an aspect sensitivity effect in spite of a radar beam tilted 20° off zenith.

Thus, complementary observations seemed to be necessary for confirming the high performances of the MU radar to measure the wind with the Doppler mode. In this paper, we show new comparisons of tropospheric and stratospheric winds measured by the MU radar and instrumented balloons. These comparisons are original,

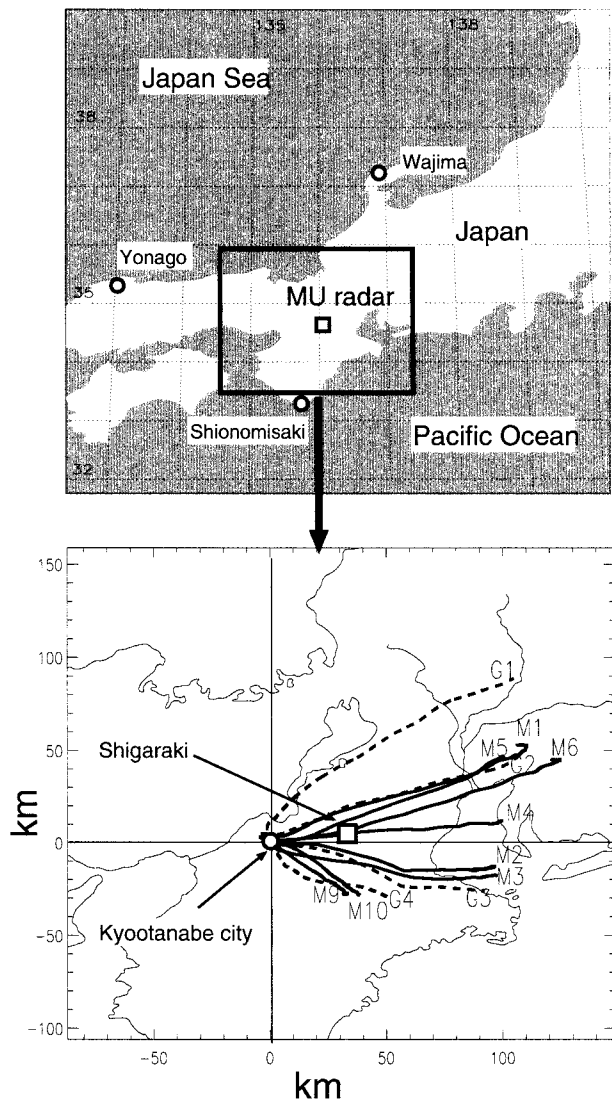


FIG. 1. (top) Positions of the MU radar observatory and meteorological stations located around the MU radar. (bottom) Trajectories of the 12 balloons used during the MUTSI campaign without failure of the GPS wind measurements. The trajectories of the 4 GPS pilot balloons and 8 MUTSI balloons are given in dashed and solid lines, respectively.

since they have been performed with global positioning system (GPS) Väisälä radiosondes (RS80G) hung below capesphere balloons (Barat and Villayes, 1998). The observations have been carried out during the French–Japanese measurement campaign called MUTSI (MU radar temperature sheets and interferometry) during 10–26 May 2000. This campaign resulted from a collaboration between the Radio Science Center for Space and Atmosphere (RASC) of Kyoto University (Japan), Laboratoire de Sondages Electromagnétiques de l’Environnement Terrestre (LSEET) of Toulon-Var University (CNRS, France), and Service d’Aéronomie (SA) of Paris VI University (CNRS, France). It consisted of launching instrumented balloons developed by SA near

the MU radar. The main objective was to collect ultra-high vertical resolution (about 8 cm) temperature profiles close to the MU radar operating in different modes (Doppler beam scanning, spatial and frequency domain interferometry). Different radar datasets were then collected during the balloon flight periods for different kinds of studies. In particular, the comparisons of the datasets are expected to give us more information on the origin of aspect sensitivity of the VHF radar echo power assumed to be produced by temperature sheets (very thin layers with steep temperature gradients) already observed by Dalaudier et al. (1994) in the free atmosphere. We also expect to obtain more details on the spatial and temporal structure of the stable sheets, their relationship with the “classical” turbulence and with the phenomena at larger scales, such as internal gravity waves. A more detailed description of the balloon equipment and experimental setup will be given in a subsequent work. In the present paper, we will restrict the description of the experiment to the purpose of the study.

Thus, in section 2, the experimental setup is first briefly described, and the comparison results and statistical analyses are described in section 3. The origin of noticeable differences between both measurements for two flights are discussed and accounted for in section 4. Comparisons with routine rawinsondes from surrounding meteorological stations (including Shionomisaki) are also shown in section 5 for interpretation of the results obtained with the MU radar by Kato et al. (1986). Finally, conclusions of this work are given in section 6.

2. Experiment description

a. Balloon experimental setup

The balloon launching site was located about 30 km westward from Shigaraki, within the Bayryo Junior High School of Kyootanabe (34°46’N, 135°47’E) (Fig. 1). This place was chosen after a climatological study of the winds over the MU radar areas (in May) over the last 10 yr for maximum likelihood that the balloons would drift over the radar at altitudes close to the tropopause.

1) GPS RADIOSONDES

Ten “capesphere” balloons (see below) carrying instrumented gondolas dedicated to ultra high-resolution temperature measurements were launched during night periods between 0000 LT (local time) and 0400 LT. Dates and times of the measurements are given in Table 2. The high-resolution instrumentation, developed by SA, will not be discussed here. Such a gondola (hereafter called MUTSI gondola) transmits data through a Väisälä RS80G radiosonde, which also provides pressure, temperature, humidity (PTU), and wind velocity measurements using the GPS navigation system. The

TABLE 2. Information on the balloons launched during MUTSI campaign.

Index number	Day	Time (LT)	GPS	BA ^a (km)	MD ^b (km)	A ^c (km)
M1	13	0040	Yes	25.70	10.5	8.3
M2	15	0012	Yes	28.30	5.5	8.5
M3	16	0220	Yes	20.43	10.5	8.4
M4	19	0014	Yes	20.70	1.0	9.9
M5	21	0006	Yes	19.31	5.5	8.1
M6	21	0258	Yes	25.67	1.8	7.1
M7	22	0034	No ^d	24.50		
M8	24	0107	No ^d	27.05		
M9	25	2311	Yes	25.98	19.4	14.3
M10	26	0220	Yes	20.06	15.8	14.1
G1	10	2230	Yes	16.55	28.7	8.5
G2	12	2145	Yes	16.75	10.8	8.1
G3	14	2126	Yes	19.20	6.8	8.6
G4	25	0005	Yes	18.92	20.4	12.7

^a Burst altitude (BA) of the balloon.

^b Minimum horizontal distance (MD) between MU radar and balloon.

^c Altitude A of the balloon corresponding to MD.

^d GPS receiver trouble.

radiosonde retransmits the position messages from GPS satellites down to the ground equipment (400 MHz Väisälä Digicora receiver), where the comparison with messages received from the same satellites on the local GPS antenna (actually located on the roof of the school) provides the relative velocity of the gondola expected to be close to that of the air mass in which the balloon is embedded. This velocity is sampled at 2 Hz and processed by the receiver software in order to produce a smoothed wind velocity “profile” with a sampling time of 10 s. The software is able to handle missing data (due to temporary bad reception conditions) and applies a smoothing to the raw velocity measurements in order to filter out spurious motions of the radiosonde, such as pendulum motion for example, and to reduce the measurement noise. This “edited” velocity profile is thus assumed to be representative of the wind conditions at the balloon level and its vertical resolution is about 50 m (for a typical ascent velocity of 5 m s^{-1}).

Four RS80G radiosondes were also launched (without MUTSI gondolas) with smaller capesphere balloons (see Table 2 for date and time). These balloons were initially dedicated to measure the wind profile in order to predict the trajectory of the MUTSI gondola launched about 2 h later. Such a trajectory prediction was motivated by safety considerations in order to avoid possible descent of the gondolas within densely populated areas. However, after an initial test period, these pilot balloons were replaced by trajectory calculations based on the MU radar wind profiles, which provided equivalent accuracy, as is shown in the present paper.

2) CAPESPHERE BALLOONS

We call capesphere a conventional meteorological (rubber) balloon covered with an extended polyethylene

cape (similar to a long “bag,” several micrometers thick and 7 m long). This cape was first used by Barat and Villaeys (1998) in order to reduce the self-induced motions of conventional meteorological balloons. According to these authors, the capesphere is a better wind sensor during its ascent than conventional balloons. The horizontal velocities deduced from GPS measurements are then representative of the atmospheric motions for all vertical scales larger than 100 m. Moreover, the drastic decrease of the balloon erratic motions also reduces the amplitude of any angular jitter induced on the vane-oriented MUTSI gondola, thus improving the quality of high-resolution measurements of the atmospheric temperature fluctuations. The cape was fixed at the upper pole of all rubber balloons. The MUTSI gondolas were hung 100 m below the balloons in order to get a suitable ventilation of the high-resolution thermometers and to avoid the turbulent wake induced by the balloon itself (Barat et al. 1984). In the case of pilot balloons, radiosondes were hung at various distances (from 10 to 30 m).

b. Radar experimental setup

During GPS pilot balloon flights, the MU radar was operated in the standard observational mode (hereafter called “STD” mode) used every month by the Radio Science Center for Space and Atmosphere (RASC) for climatology studies. It consists of a 5-beam Doppler mode giving measurements from 0.15 km up to a 24.15-km distance at 150-m range resolution. In fact, the lowest observable height in STD mode is 2.1 km due to the receiver recovery time. The beams are steered every interpulse period (IPP) in vertical and at 10° from zenith toward north, east, south, and west. A wind profile is obtained every ~ 1 min. A first observational mode allows us to collect data from 5.1 to 24.15 km and a second one from 0.15 to 19.6 km. The composite profile from 0.15 to 24.15 km is obtained every ~ 2 min.

During the MUTSI gondola flights, different radar configurations were used, interleaved with a simultaneous Doppler/Spaced Antenna mode, hereafter called “MUTSI mode,” common to all radar measurement periods. In particular, this observational mode will permit us to apply Doppler and SA methods for further studies. The altitudes were sampled from 4.2 to 23.75 km with a range resolution of 150 m in 5 directions (1 vertical and 4 oblique beams) steered at 15° from the zenith. In order to compensate for a possible loss of sensitivity of the radar in oblique directions due to a larger zenith angle with respect to the STD mode (15° instead of 10°), a larger number of coherent integration was applied. Moreover, because the beam was steered after time series acquisition in each direction, it also theoretically leads to a better sensitivity of the radar at high altitudes (see Table 3) in detriment to simultaneous data acquisition in each beam direction. It took ~ 2 min 10 s for

TABLE 3. Radar parameters for the MUTSI and STD modes (see text for details).

Parameter	MUTSI	STD
Interpulse period (μs)	400	400
Subpulse duration (μs)	1	1
Range resolution (m)	150	150
Ngate	128	161
Direction number %*	5	5
Zenith angle ($^\circ$)	15	10
Receiving array number	4	1
Coherent integration (vertical)	256	36
Coherent integration (oblique)	128	36
Incoherent integration	— (time series)	6
Nyquist frequency (Hz, vertical)	4.88	6.51
Nyquist frequency (Hz, oblique)	9.76	6.51
V_r aliasing (m s^{-1} vertical)	15.72	21.0
V_r aliasing (m s^{-1} oblique)	31.44	21.0
Trecord (s vertical)	26.2	58.9 (total)
Trecord (s oblique)	13.1	58.9 (total)
G (SNR) ⁺ (dB vertical)	+8.3	—
G (SNR) ⁺ (dB oblique)	+5.3	—
G (D) ⁺ (dB vertical)	+6.8	—
G (D) ⁺ (dB oblique)	+1.4	—

* Beam steered after collecting time series in a given direction for the MUTSI mode.

⁺ G is the gain of SNR (dB) and detectability (D) (without incoherent integration) with respect to the STD mode observations.

the acquisition of a wind profile, and its calculation was performed every ~ 5 min.

Table 3 summarizes the main parameters used for the STD and MUTSI modes. A statistical analysis of the results for 10° and 15° zenith angles permitted us to study the effect of zenith angle on the wind estimates with the MU radar.

3. Results and statistical analyses

Balloon trajectories during the ascent period from the ground until their burst height are shown in Fig. 1 for the 12 flights when the GPS measurements are available. The balloons took ~ 70 min to reach ~ 20 -km altitude. The numbers M1 to M10 and G1 to G4 indicated on the figure for each trajectory correspond to the flight names given in Table 2. The maximal and minimal horizontal distances between a balloon and the radar site during its ascent were less than ~ 120 and 1 km, respectively. Most of them drifted close over the MU radar (less than 20 km) in the higher troposphere or close to the tropopause because of the dominant eastward wind component.

Figure 2 shows vertical profiles of mean meridional and zonal components of the winds measured by the MU radar corresponding to the periods of the 12 successful balloon flights (8 launches performed during the MUTSI mode are shown in Figs. 2a and 2b, and 4 launches during the STD mode are shown in Figure 2c). The radial velocities used for the horizontal wind estimation correspond to the average of the two values measured with opposite beams. The profiles have been

averaged over about 70 min from the balloon launch time. Before averaging, each radar profile has been processed by using an algorithm, suppressing aberrant values produced by airplanes and electromagnetic interferences or absence of signals. This algorithm consisted of applying simple spatial and time continuity criteria. A value was considered nonphysical if the wind difference between two consecutive radar gates was larger than 5 and 3 m s^{-1} for the MUTSI and STD mode, respectively. A pair of arbitrary thresholds was used because of the different radar configurations. Moreover, each 70-min averaged point of the radar profile has not been calculated with the same number of points, depending on the presence of outliers or not.

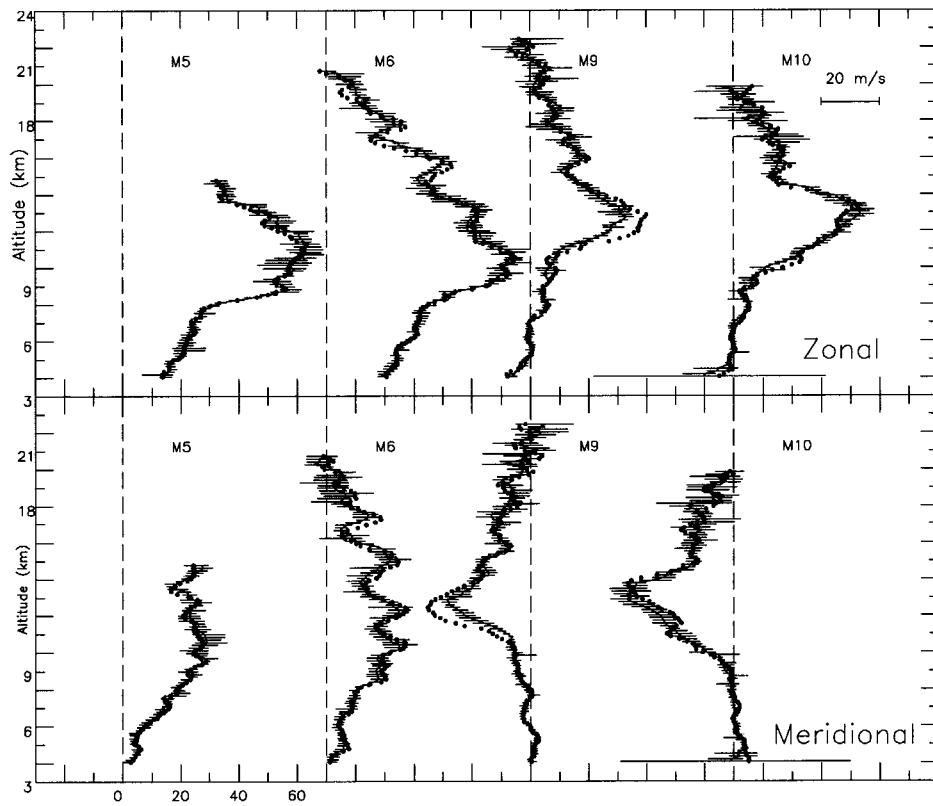
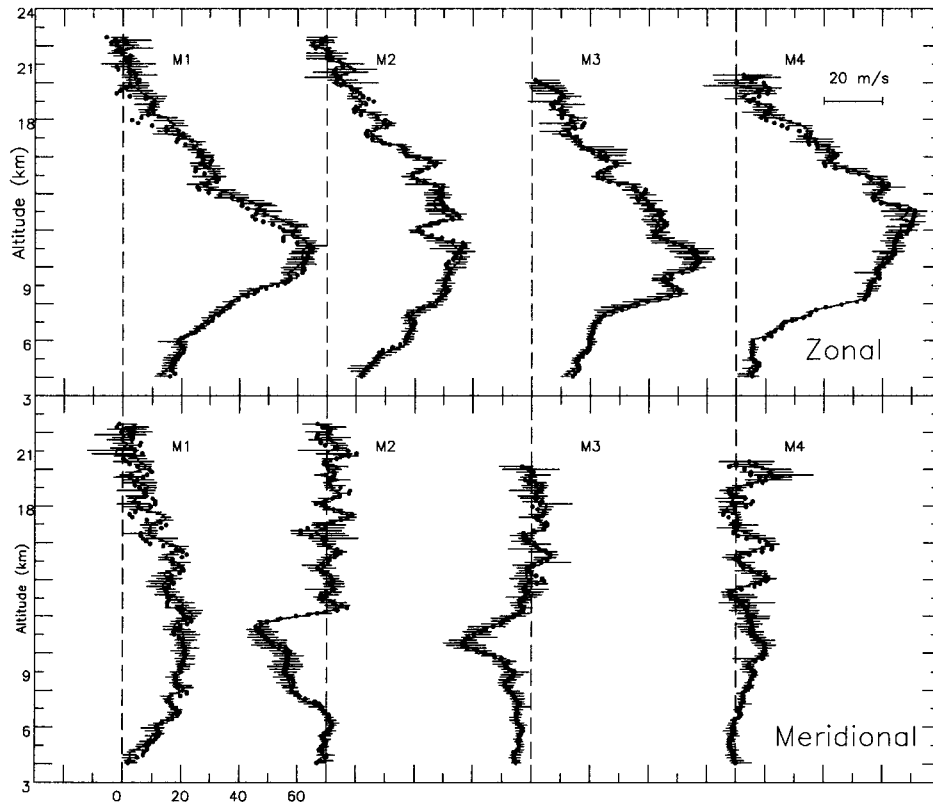
The horizontal bars give the range of the values used for the average calculation after removing aberrant values. When the radar signal-to-noise ratio (SNR) is large, the estimation errors are expected to be much smaller than the wind variability (Yamamoto et al. 1988). The horizontal bars thus mainly indicate the variability of the wind field during this 70-min period for most altitudes. However, a larger variability above ~ 18 km results from a low SNR (see, e.g., Fig. 2a) and is then not representative of the wind fluctuations. It is important to note that this variability and thus the mean value can depend on the algorithm used for suppressing the aberrant values.

Also shown in Figs. 2a–c are the meridional and zonal components of the wind measured by the 12 GPS radiosondes (chain of circles). Each profile has been first resampled at a constant vertical step of 50 m (using a cubic spline interpolation) and smoothed with a suitable Gaussian window corresponding to the power radar weighting function in order to get a 150-m sampling at the altitudes of the radar gates. Except for flights M9 (where the radar underestimates the jet-stream by 10 – 15 m s^{-1}), the comparison between the two kinds of profiles is excellent. The balloon-deduced profiles are almost always contained within the region defined by the horizontal bars.

It is extremely noteworthy that even the wavy structures that clearly appear almost every day, especially in the meridional wind, are seen by both instruments with a good coincidence in altitude and amplitude. To our knowledge, this is the first time that such structures are so clearly defined by simultaneous balloon and VHF radar techniques with a 150-m range resolution.

Statistical analyses and discussion

Figures 3 and 4 show statistical analyses for the datasets collected with MUTSI and STD modes, respectively. The data collected during M9 and M10, which show significant wind differences (≈ 10 – 15 m s^{-1}), are not included in Fig. 3 and will be analysed in section 4. Moreover, the measurements between 0.15 and 2.1 km available for the STD mode have not been used



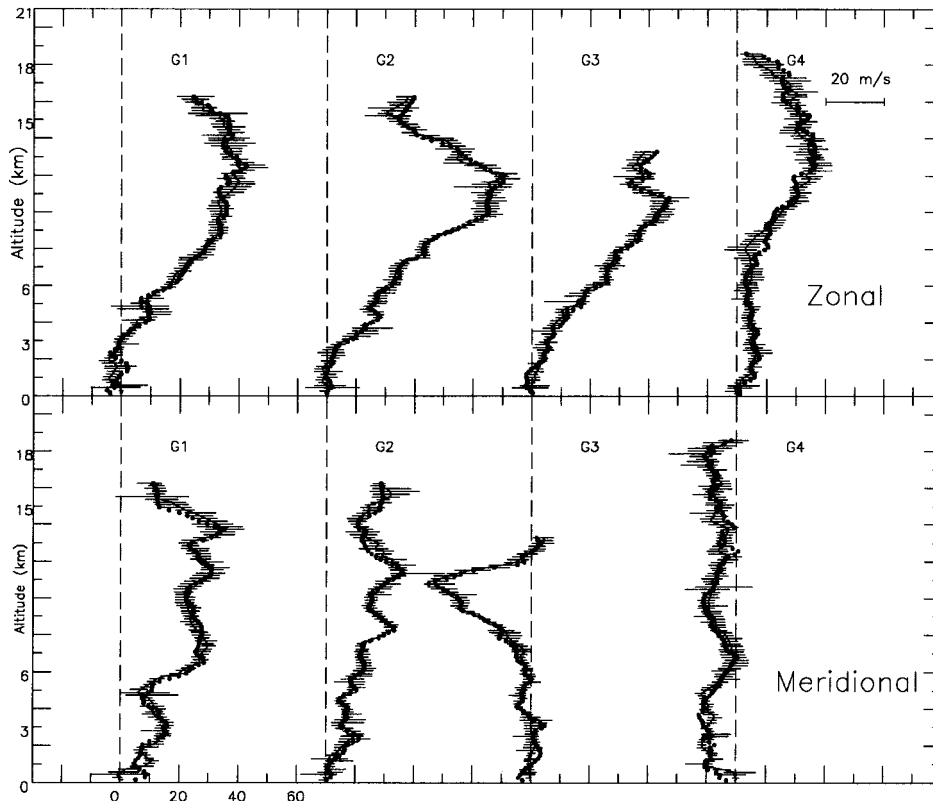


FIG. 2. (Continued)

because the radar is not reliable within this altitude range.

First, in Figs. 3a and 4a, the radar-deduced zonal and meridional wind components are plotted against those measured by GPS radiosondes. Differences appear when the points do not lie on the diagonal. These differences result from a combination of estimation errors, sample acquisition methods, and spatio-temporal inhomogeneities. However, we did not find any systematic bias in the comparisons, since the linear regression curves have a slope and intercept very close to 1 and 0, respectively (see Table 4).

The differences between the meridional components are plotted versus the differences of the zonal components in Figs. 3b and 4b. A point at the center of the graph indicates that there is no difference between both components. The mean values of the differences are close to 0: -0.15 and 0.55 m s^{-1} for the zonal component in MUTSI and STD modes, respectively, and 0.24 and -0.18 m s^{-1} for the meridional component,

indicating also that the overall datasets are not affected by instrumental or geophysical biases. Table 4 shows the standard deviations of the differences of the 2 wind components are $2.52\text{--}2.70 \text{ m s}^{-1}$ in MUTSI mode (without M9 and M10) and $1.92\text{--}2.04 \text{ m s}^{-1}$ in STD mode. The corresponding values for the modulus are 3.7 and 2.8 m s^{-1} , respectively. It is difficult to conclude if the better accuracy with the STD mode is significant or not because of the small number of cases. It can also be an effect of the different data acquisition methods and/or an effect of the data processing used for excluding aberrant values.

The effects of SNR on the differences between the zonal and meridional components are shown in Figs. 3c and 4c. For this analysis, the averaged values of SNR observed in the four oblique beams are used. The SNR effects are particularly noticeable for the MUTSI mode, where the largest differences are observed when SNR is small; the variability becomes significantly larger for $\text{SNR} < 0 \text{ dB}$ and is maximum near the noise level

←

FIG. 2. (a) Comparisons between the radar (solid lines) and GPS (chain of circles) meridional (bottom) and zonal (top) wind components for M1, M2, M3, and M4. The horizontal bars indicate the variability (and in some less extent the estimation errors) of the wind data used for the averaging calculation. (b) Same as (a) for M5, M6, M9, M10 in MUTSI mode. The GPS measurements above $\approx 15 \text{ km}$ are not available for M5. (c) Same as previously for G1, G2, G3, and G4 in STD mode. The results between 0.15 and 2.1 km are shown for information even if the radar measurements are not reliable. The GPS measurements above $\approx 13.5 \text{ km}$ are not available for G3.

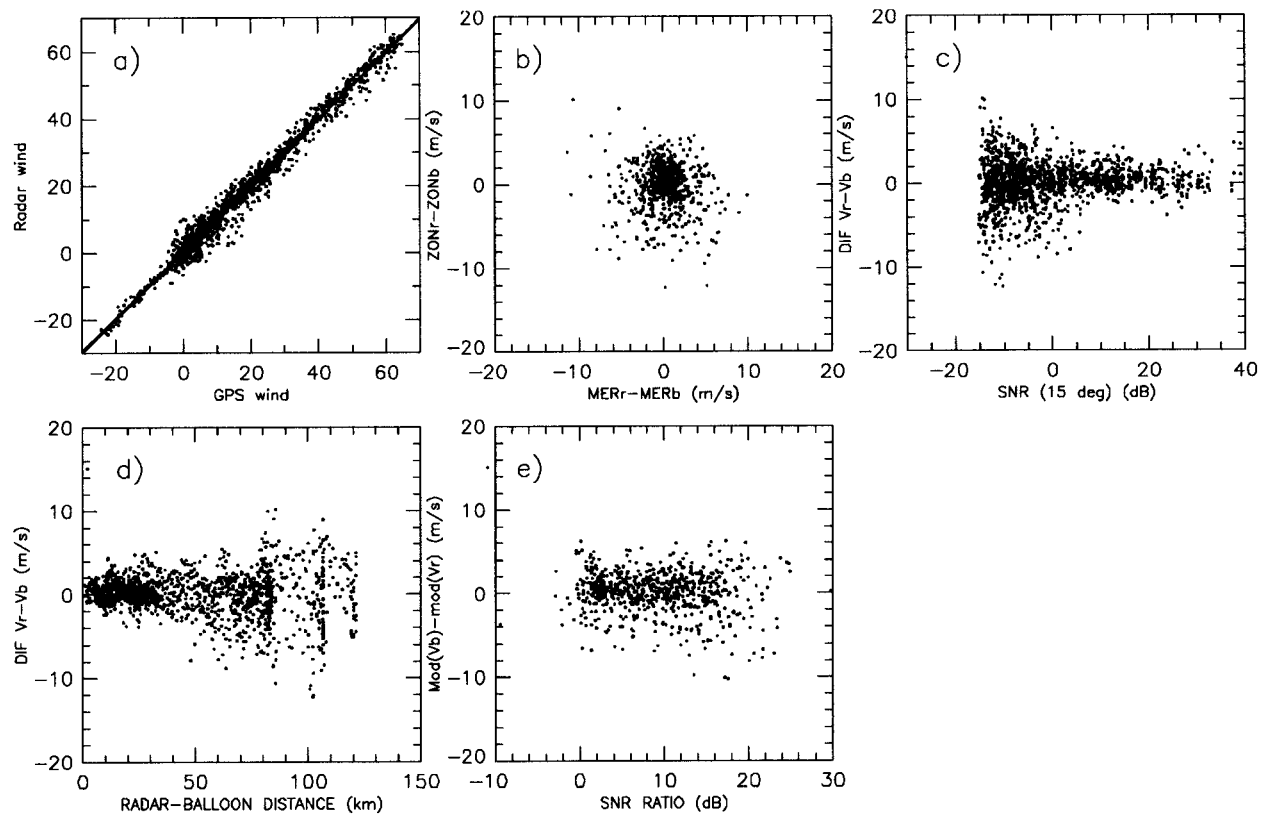


FIG. 3. (a) Zonal and meridional wind components (m s^{-1}) measured by GPS radiosondes vs those deduced from MU radar measurements in MUTSI mode (see text). The scatterplot is given for M1, M2, M3, M4, M5, and M6. Statistics are given in Table 4. (b) Differences (m s^{-1}) between MU radar and GPS wind component measurements corresponding to the datasets shown in (a). The differences between the meridional and zonal components are given by the horizontal and vertical coordinates, respectively. (c) Wind component differences vs radar signal-to-noise ratio measured in oblique direction (15° off zenith). (d) Wind component differences vs the horizontal distance between radar and balloons. The accumulation of points for some horizontal distances (80, 105, 120 km, . . .) is the consequence of vanishing winds above the subtropical jet, leading to a nearly constant distance from the radar. (e) Differences between the radar-deduced and radiosonde wind velocities vs the ratio of vertical and oblique radar echo powers (aspect sensitivity).

(~ -15 dB), but this variability also depends on the efficiency of the data processing algorithm used for suppressing aberrant values. However, it is worth noting that the differences become significantly smaller for large SNR. In Fig. 5, the standard deviation of the differences for both zonal and meridional components are shown versus minimum SNR (dB) for the MUTSI mode. As expected, the standard deviation decreases as SNR threshold increases. A minimum is reached from 4 dB ($\sim 1.4 \text{ m s}^{-1}$), indicating that the differences cannot be attributed anymore to SNR effects. From Fig. 4c, it seems that the SNR effects are not so important in STD mode, but the noise level (~ -20 dB) was not reached for the presented comparisons, and some significant differences for $\text{SNR} < 0$ dB are found.

The effects of the horizontal distance between MU radar and balloons (horizontal variability) are presented in Figs. 3d and 4d. As expected, the smallest average differences are observed when the radiosonde is close to the radar. The range of the cloud of points appears to grow as the distance increases. However, due to the configuration of the experiment and for most cases, a

small horizontal distance also corresponds to a large SNR. For example, at the altitudes where the SNR is larger than 10 dB in MUTSI mode, the horizontal distance is always smaller than 40 km. Reciprocally, a large distance corresponds to a small SNR. The consequence is that the minimum standard deviation obtained in Fig. 5 ($\sim 1.4 \text{ m s}^{-1}$) is approximately reached for any SNR threshold if the radar-balloon horizontal distance is limited to 50 km. Consequently, it is difficult to separate the effects of the radar-balloon distance and SNR on the increase of wind differences.

Finally, in Figs. 3e and 4e are the differences of the speed (modulus) $|V_b| - |V_r|$ versus the ratio of radar echo power in vertical and oblique beams P_v/P_o (radar aspect sensitivity). If wind speed modulus is underestimated by the radar in the case of strong aspect sensitivity, the observed difference is expected to be positive and its magnitude proportional to the aspect sensitivity because the effective oblique beam direction is closer to the zenith than the real beam pointing direction. However, Figs. 3e and 4e clearly indicate (to our surprise) that the differences do not depend on aspect sen-

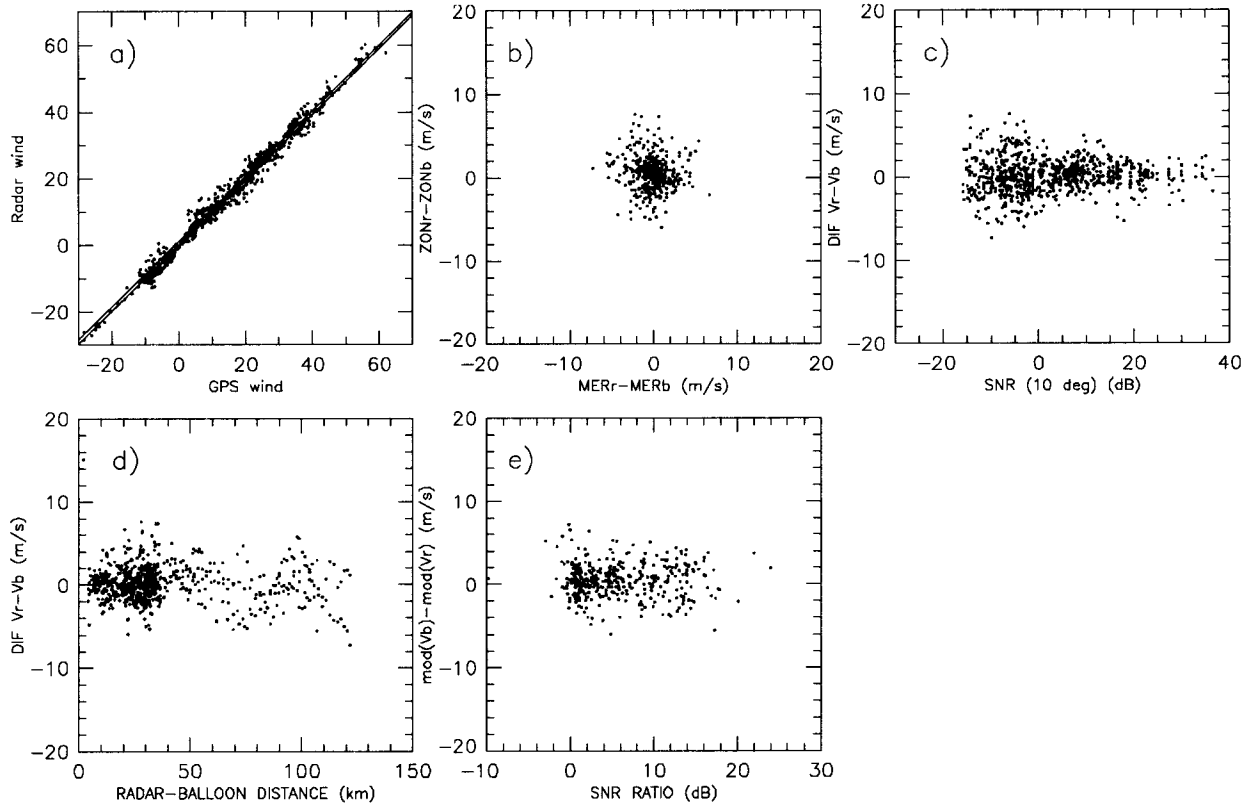


FIG. 4. Same as Fig. 3 for G1, G2, G3, and G4 in STD mode (see caption of Fig. 3 for more details).

sitivity estimated from data collected at 15° (MUTSI mode) or even 10° (STD mode). This result is at variance with previous theoretical or experimental studies such as those presented by Hocking et al. (1990) or by Kishore et al. (2000), for example. However, it is in agreement with the observations presented with the MU radar by Tsuda et al. (1986), which showed that the wind estimates are equivalent when using beams tilted by 8°

or 10° off zenith, indicating that the aspect sensitivity effects can be neglected for equivalent or larger tilt angles.

According to physical considerations, an effective pointing angle θ_{eff} must be used instead of the beam tilt angle θ when we derive the horizontal wind from the radial measurements. Using Hocking et al.'s (1990) model and MU radar parameters, we obtained for a typ-

TABLE 4. Statistical comparisons between radar and GPS radiosonde wind component measurements for different datasets.

Data	Comp.	Pairs	Mean ^a	(σ_{rms}) ^b	Intercept ^c	Slope ^d
M1 ... M10	Mer.	911	0.10 ± 0.13	2.76	0.07 ± 0.18	0.988 ± 0.010
	Zon.	911	0.13 ± 0.14	2.86	0.41 ± 0.32	1.009 ± 0.014
M1 ... M6	Mer.	673	0.24 ± 0.14	2.52	0.32 ± 0.22	0.985 ± 0.018
	Zon.	673	-0.15 ± 0.15	2.70	-0.19 ± 0.40	1.001 ± 0.012
G1 ... G4	Mer.	384	-0.24 ± 0.14	1.92	1.00 ± 0.19	0.986 ± 0.006
	Zon.	384	0.57 ± 0.15	2.04	-0.16 ± 0.10	0.981 ± 0.007
M1 ... M6	Mer.	155	0.34 ± 0.15	1.27	0.19 ± 0.20	1.039 ± 0.022
SNR > 10 dB	Zon.	155	0.56 ± 0.15	1.31	0.46 ± 0.52	1.004 ± 0.020
M1 ... M6	Mer.	350	0.28 ± 0.10	1.31	0.27 ± 0.14	1.003 ± 0.012
D° < 50 km	Zon.	350	0.55 ± 0.12	1.61	0.65 ± 0.40	0.997 ± 0.010

^a Average (m s^{-1}) of the differences. The 90% confidence interval is calculated using the relation $2\sigma_{\text{rms}}/\sqrt{N/2}$ where N is the number of pairs and $N/2$ is the number of independent samples.

^b RMS deviation (m s^{-1}) of the differences of zonal and meridional wind components.

^c Intercept of the least squares fit line with the 90% confidence interval (statistical error for a Gaussian model).

^d Slope of the least squares fit line with the 90% confidence interval (statistical error for a Gaussian model).

^e Horizontal distance D between radar and balloons.

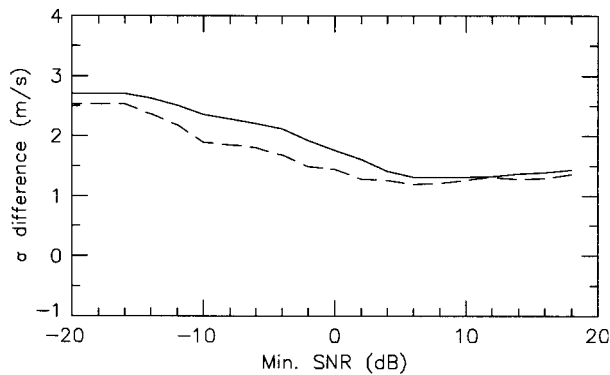


FIG. 5. Standard deviation of the differences between the zonal (solid lines) and meridional (dashed lines) components measured with the MU radar in MUTSI mode and GPS radiosondes versus oblique SNR threshold.

ical P_v/P_o ratio of 20 dB in the lower stratosphere effective angles of 8.3° and 13.9° instead of 10° and 15° , respectively. Underestimates of 20% and 8% of the wind speed modulus could arise, for example, 10 and 4 m s^{-1} , respectively, for a speed of 50 m s^{-1} if the radar beam zenith angle is used. Thus, a significant wind speed underestimate is predicted for large velocities with 10° due to aspect sensitivity effects. However, the results of our comparisons do not show any bias. It is particularly the case for the case G2 (Fig. 2c), for example, for which the zonal wind profile measured by both techniques agree very well and the speed is larger than 50 m s^{-1} at altitudes where the power ratio is about $\sim 15\text{--}20$ dB (not shown). This disagreement between the model and observations may result from the fact that the model does not account for an isotropic (or even nearly isotropic and maybe turbulent) backscattering background. Thus, in light of these results, it seems preferable not to apply the effective pointing angle for a radar system with a small beamwidth like the MU radar when $\theta \geq 10^\circ$. However, for aspect sensitivity stronger than observed during MUTSI, the aspect sensitivity effect may be more important. It also may be more important for a VHF wind profiler with a larger beamwidth.

4. Analyses of M9 and M10

The wind conditions during M9 and M10 are extremely different from those observed during the other observation periods (Figs. 2a,b). For these conditions, the comparison results are not so good. Indeed, the profiles obtained during the flight M9 show a significant difference around the jet stream (centered around $\sim 12 \text{ km}$ altitude). The radar-deduced wind profile is smaller than the wind measured by the balloon by $10\text{--}15 \text{ m s}^{-1}$. Obviously, the introduction of this case in the previous statistics would lead to a degradation of the results (see Table 4). It is inter-

esting to note that this discrepancy cannot be explained by aspect sensitivity even if the previously mentioned theory is used. Indeed, a correction of about $+2.4 \text{ m s}^{-1}$ (i.e., much smaller than the observed difference) should be applied on the radar wind profile for $\theta = 15^\circ$, $V_{\text{max}} = 30 \text{ m s}^{-1}$ and $P_v/P_o = 20$ dB. Moreover, it is also useful to note that the profiles M10 measured about 3 h after M9 show opposite feature at the same altitude range: the radar-deduced wind velocity is larger than the radiosonde-measured one by $\sim 5 \text{ m s}^{-1}$, mainly resulting from a temporal increase of the wind velocity measured by the radar (Fig. 6). A better agreement would be found around the jet-stream altitude between the radiosonde wind profile obtained during M9, with the wind measured by the radar 3 h later during M10. These observations strongly suggest that the differences between the two kinds of profiles result from a strong horizontal inhomogeneity of the wind field. This hypothesis is confirmed by meteorological analyses that show a slow advection of the core of the jet stream approximately toward the north, related to the passage of a warm front during the night of 25 May.

5. Discussion of the effects of the “noncolocalization” of the measurements

Figure 7 gives some examples of the effects of the distance on the quality of the comparisons. Other comparisons have been performed between winds measured with the MU radar in STD mode and the ones measured from routine rawinsondes launched every day at 1200 UTC (2100 LT) at 3 meteorological stations (Shionomisaki, $33^\circ 27' \text{N}$, $135^\circ 46' \text{E}$; Yonaga, $35^\circ 26' \text{N}$, $133^\circ 2' \text{E}$; Wajima, $37^\circ 23' \text{N}$, $136^\circ 54' \text{E}$) (see Fig. 1) located at approximately 170, 380, and 350 km from the radar site, respectively. The radar profiles plotted in Fig. 7 have been obtained after 1-h averaging between 2100 and 2200 LT (since the variability of the measurements during the 1-h averaging is of the same order as those shown in Fig. 2, the horizontal bars are not indicated for the clarity of the figure). The vertical resolution of the rawinsonde profiles is very coarse compared to that of the GPS radiosondes and depends on height.

These comparisons are similar to those presented by Kato et al. (1986). As already shown by these authors, the overall comparisons are fairly good, but there are some noticeable differences that can be unambiguously attributed to the distance between the location of the instruments in light of the very good agreement between “better collocated” GPS-radar comparisons. However, contrary to Kato et al. (1986), some cases exhibit radar-deduced jet-stream speeds smaller than those measured by the rawinsondes, and other cases present the opposite feature. Generally, the best comparisons at the jet-stream height are obtained with the measurements made at Yonaga, since the meteorolog-

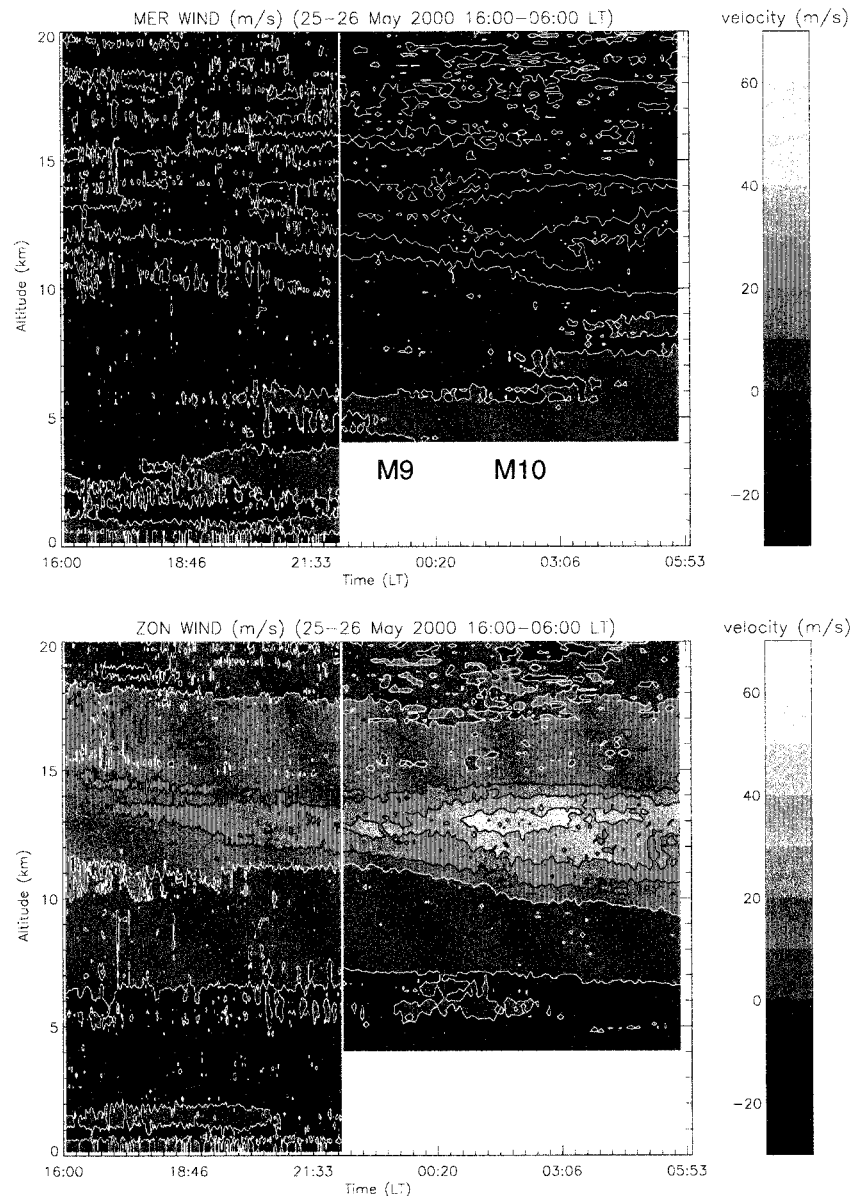


FIG. 6. (Top) Contour plot of the meridional wind component during the MUTSI observations for 25 May 2000, ~1600–0600 LT. (Bottom) Contour plot of the zonal wind component for the same period. Before 2210 LT, the measurements have been performed with the STD mode and after 2211 LT with the MUTSI mode. “M9” and “M10” approximately indicate the time of balloon launches.

ical station has a latitude similar to the MU radar observatory and the jet stream mainly varies with latitude over Japan on these days.

6. Conclusions

In this work, wind profiles measured by the VHF MU radar within the lower atmosphere up to ~20 km are compared with those deduced from GPS radiosondes launched at ~30 km westward from the radar site. These

profiles have been obtained during the MUTSI campaign, which will be described in more detail in future papers. The measurements have been carried out over a distance of ~100 km and a duration of ~1 h. Because the GPS radiosondes have been hung below capesphere-type balloons, better estimates of the wind vector (with respect to classical weather balloons) are obtained. At a 150-m range resolution, a very good agreement is obtained between the radar and balloon-deduced winds. Even the small scale wind wavy fluctuations (vertical

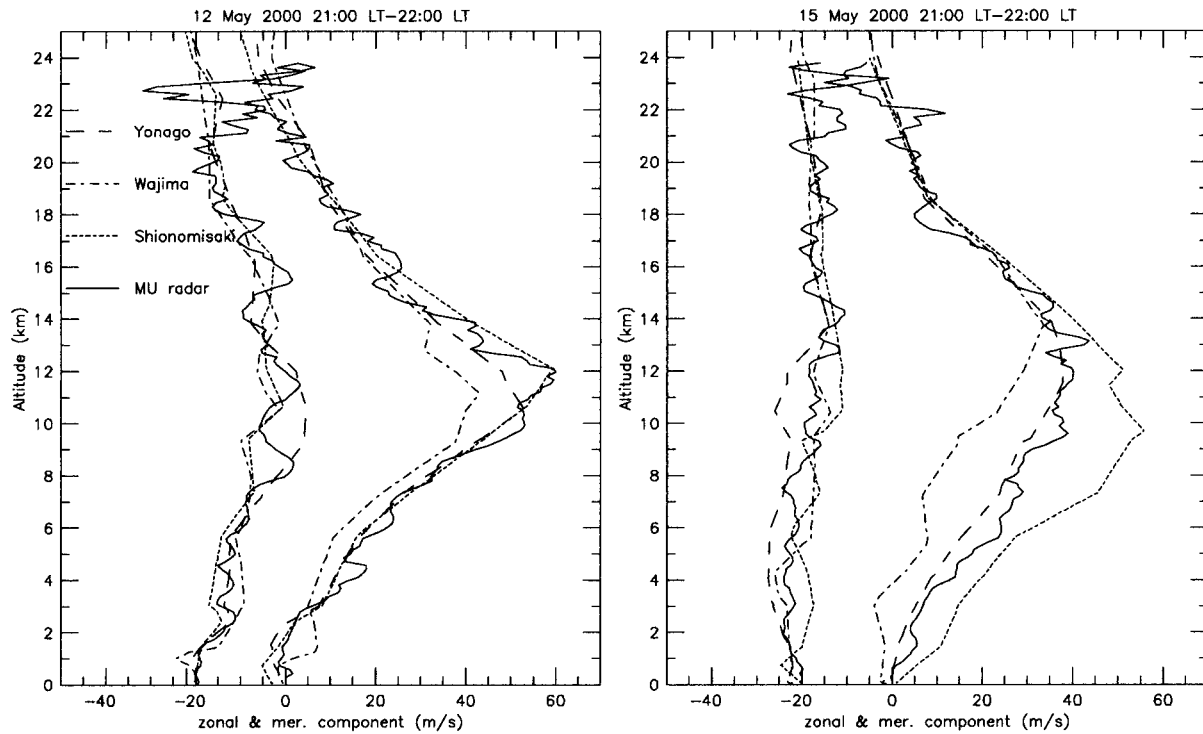


FIG. 7. Examples of comparisons of the radar and routine rawinsonde meridional and zonal wind components. For the clarity of the figure, the meridional profiles (left of the figures) have been translated by -20 m s^{-1} , and the variability of the radar wind data used for the averaging calculation are not shown. The rawinsonde data have been collected at Shionomisaki, Yonago, and Wajima (see text). It is interesting to note that rawinsondes cannot detect the well-defined wavy structures observed with the MU radar.

wavelength smaller than 1 km) associated with gravity waves are seen by both instruments generally at similar altitudes and with very similar amplitudes. The standard deviation between the differences of meridional and zonal winds are smaller than 2.7 m s^{-1} (if M9 and M10 are excluded), and no bias has been found except for one case that could be explained by particular meteorological conditions.

The following conclusions can be made.

- 1) The MU radar is particularly efficient for measuring the wind field, with very high accuracy at a 150-m range resolution, by using the Doppler mode with tilted beams at 15° and also at 10° , as commonly used by RASC. Using the reasonable hypothesis that both instruments are not affected by the same kind of biases, we can conclude reciprocally that the capsphere balloons equipped with GPS radiosondes are very accurate for measuring the wind field.
- 2) As expected, the largest differences between the measured winds are found when the SNR is small (instrumental effect) and when the radar-balloon distance is large (horizontal wind inhomogeneity effect) even if it is difficult to deduce which of these two parameters dominates the present datasets. The standard deviation of the differences can be as small as 1.5 m s^{-1} for $\text{SNR} > 0 \text{ dB}$ and when the horizontal separation between the instruments is smaller than
- 3) More unexpected, in light of investigations with other wind profilers, is the “nonsensitivity” (in a statistical sense) of the MU radar-deduced winds to aspect sensitivity. Indeed, this work seems to confirm that a narrow radar beam tilted 10° off zenith is sufficient for avoiding the effects of aspect sensitivity. However, some effects might produce wind speed underestimates at some altitudes, but these affects are not significant within the present analysis.
- 4) Comparisons with routine rawinsondes show large differences that can be fully interpreted in terms of the large horizontal distance between the measurement locations. This confirms the conclusion of Kato et al. (1986) regarding the effects of the horizontal inhomogeneity on the quality of the comparisons with the MU radar wind profiles.

Acknowledgments. The balloon operations of the MUTSI campaign was mainly supported by CNES (Centre National d’Etudes Spatiales) of France. We wish to thank Dr. M. Ishihara from the Observation Department of the Japan Meteorological Agency and Mr. E.

Maeda from the Japan Weather Association for their collaboration in balloon launching. We would like also to thank N. Kawano and K. Kubo for their help during the campaign, Mr. J. C. Genie from Service d'Aeronomie, and Mr. P. Bombezin and Mr. B. Dartiguelongue from CNES for their contribution. Finally, we also thank Prof. M. Crochet (LSEET) for his helpful comments concerning the elaboration of this manuscript. This paper was prepared and accomplished while one of the authors (H. L.) was a Lavoisier Grant (Ministry of Foreign Affairs, France) and a Japan Society for the Promotion of Science (JSPS) postdoctoral fellow at the Radio Science Center for Space and Atmosphere (RASC). The MU radar belongs to, and is operated by, the Radio Science Center for Space and Atmosphere, Kyoto University.

REFERENCES

- Astin, I., and L. Thomas, 1992: The accuracy and precision of radar wind measurements. *Proc. Fifth Workshop on Technical and Scientific Aspects of MST Radar*, Aberystwyth, Wales, STEP, 15–20.
- Barat, J., and J. Villaeys, 1998: How to take advantage of the GPS resolution with meteorological balloons. Preprints, *10th Symp. on Meteorological Observations and Instrumentation*, Phoenix, AZ, Amer. Meteor. Soc., 55–57.
- , C. Cot, and C. Sidi, 1984: On the measurement of the turbulence dissipation rate from rising balloons. *J. Atmos. Oceanic Technol.*, **1**, 270–275.
- Campistron, B., Y. B. Pointin, F. Lohou, and J. P. Pagés, 1999: Aspect sensitivity of VHF radar echoes observed in the middle and upper troposphere during the passage of a cut-off low. *Radio Sci.*, **34**, 667–680.
- Chadwick, R. B., 1985: Wind profiler demonstration system. *URSI/SCOSTEP Workshop on Technical and Scientific Aspects of MST Radar*, URSI/SCOSTEP, 336–337.
- Chang, N. J., 1980: Precision of tropospheric/stratospheric winds measured by the Chatanika radar. *Radio Sci.*, **15**, 371–382.
- Crane, R. K., 1980: Radar measurements of wind at Kwajalein. *Radio Sci.*, **15**, 383–394.
- Dalaudier, F., C. Sidi, M. Crochet, and J. Vernin, 1994: Direct evidence of “sheets” in the atmospheric temperature field. *J. Atmos. Sci.*, **51**, 237–248.
- Ecklund, W. L., D. A. Carter, and B. B. Balsley, 1979: Continuous measurement of upper atmospheric winds and turbulence using a VHF Doppler radar: Preliminary results. *J. Atmos. Terr. Phys.*, **41**, 983–994.
- Fukao, S., T. Sato, N. Yamasaki, R. M. Harper, and S. Kato, 1980: Radar measurement of tidal winds at stratospheric heights over Arecibo. *J. Atmos. Sci.*, **37**, 2540–2544.
- , K. Aoki, K. Wakasugi, T. Tsuda, S. Kato, and D. A. Fleisch, 1981: Some further results on the lower stratospheric winds and waves over Jicamarca. *J. Atmos. Terr. Phys.*, **43**, 649–661.
- , T. Sato, N. Yamasaki, R. M. Harper, and S. Kato, 1982: Winds measured by a UHF Doppler radar and rawinsondes: Comparisons made on twenty-six days (August–September 1977) at Arecibo, Puerto Rico. *J. Appl. Meteor.*, **21**, 1357–1363.
- , —, P. T. May, T. Tsuda, and S. Kato, 1988: A systematic error in MST/ST radar wind measurement induced by a finite range volume effect. I. Observational results. *Radio Sci.*, **23**, 59–73.
- Hocking, W. K., 1997a: Strengths and limitations of MST radar measurements of middle-atmosphere winds. *Ann. Geophys.*, **15**, 1111–1122.
- , 1997b: System design, signal-processing procedures, and preliminary results for the Canadian (London, Ontario) VHF atmospheric radar. *Radio Sci.*, **32**, 687–706.
- , S. Fukao, T. Tsuda, M. Yamamoto, T. Sato, and S. Kato, 1990: Aspect sensitivity of stratospheric VHF radio wave scatterers, particularly above 15-km altitude. *Radio Sci.*, **25**, 613–627.
- Kato, S., T. Tsuda, M. Yamamoto, T. Sato, and S. Fukao, 1986: First results obtained with a middle and upper atmosphere (MU) radar. *J. Atmos. Terr. Phys.*, **48**, 1259–1267.
- Kishore, P., K. K. Reddy, D. N. Rao, P. B. Rao, A. R. Jain, G. V. Rama, and S. Sankar, 2000: A statistical comparison of Indian ST radar and rawinsonde wind measurements. *Indian J. Radio Space Phys.*, **29**, 102–114.
- Larsen, M. F., 1983: Can a VHF Doppler radar provide synoptic wind data? A comparison of 30 days of radar and radiosonde data. *Mon. Wea. Rev.*, **111**, 2047–2057.
- Pauley, P., R. L. Creasey, W. L. Clark, and G. Nastrom, 1994: Comparisons of horizontal winds measuring by opposing beams with the Flatland radar and between Flatland measurements and NMC analysis. *J. Atmos. Oceanic Technol.*, **11**, 256–274.
- Röttger, J., 1981: Investigations of lower and middle atmosphere dynamics with spaced-antenna drift radars. *J. Atmos. Terr. Phys.*, **43**, 277–292.
- Strauch, R. G., B. L. Weber, A. S. Frisch, C. G. Little, D. A. Merritt, K. P. Moran, and D. C. Welsh, 1987: The precision and relative accuracy of profiler wind measurements. *J. Atmos. Oceanic Technol.*, **4**, 563–571.
- Tsuda, T., T. Sato, K. Hirose, S. Fukao, and S. Kato, 1986: MU radar observations of the aspect sensitivity of backscattered VHF echo power in the troposphere and the lower stratosphere. *Radio Sci.*, **21**, 971–980.
- Weber, B. L., and D. B. Würtz, 1990: Comparisons of rawinsonde and wind profiler radar measurements. *J. Atmos. Oceanic Technol.*, **7**, 157–174.
- Yamamoto, M., T. Sato, P. T. May, T. Tsuda, S. Fukao, and S. Kato, 1988: Estimation error of spectral parameters of MST radars obtained by least squares fitting method and its lower bound. *Radio Sci.*, **23**, 1013–1021.